energy&fuels

pubs.acs.org/EF

Article

Liquid Chromatographic Separation and FT-ICR MS of Crude Oils: Insights from Polar Fractions

Nerilson Marques Lima, Hugo Gontijo Machado, Gesiane da Silva Lima, Joveilton Batista da Silva Junior, Juliene Aljahara Sousa Cardoso, Gabriel Franco dos Santos, Andrea Rodrigues Chaves, Rodrigo Cabral da Silva, Alexandre de Andrade Ferreira, and Boniek Gontijo*

Cite This: *Energy Fuels* 2025, 39, 20199−20212

Read Online

ACCESS | Metrics & More | Article Recommendations | Supporting Information

ABSTRACT: Molecular characterization of petroleum and reservoir fluids is fundamental to the oil exploration and production sector. However, the complexity of the sample has been an analytical challenge, requiring modern analysis techniques such as ultrahigh-resolution mass spectrometry techniques integrated with chromatographic separation systems. The focus of this study was the detailed molecular characterization of the polar fraction of crude oils, supported by chromatographic fractionation to improve class identification and support geochemical interpretation. Chromatographic fractionations were conducted using H-MPLC, followed by characterization using ESI (±) and APPI (+) FT-ICR MS. Polar compounds from ten Brazilian crude oils were separated into six fractions (low polarity-LP, low medium polarity-LMP, high medium polarity-HMP, high polarity-HP, basic-BAS, acidic-ACD). Molecular profiles through ESI (±) and APPI (+) FT-ICR-MS allowed for the characterization of geochemical processes, formation mechanisms, and the discrimination of oils based on their origin classification and thermal evolution.

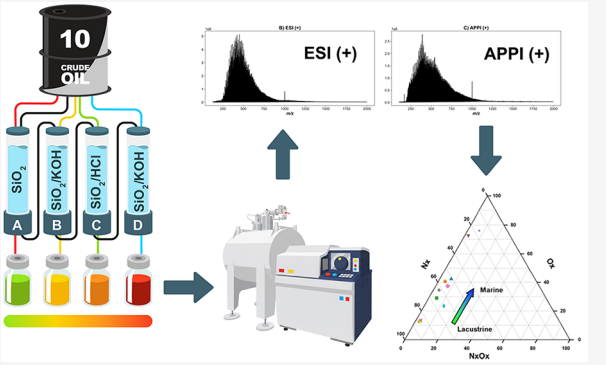

1. INTRODUCTION

The molecular analysis of petroleum and reservoir fluids and the geological, mineralogical, and chemical characterization of the components within the petroleum system are cornerstones of the oil exploration and production sector. In the drive toward a circular economy and carbon neutrality, a molecular understanding of energy production and pollutant mitigation is increasingly vital. Beyond reducing operational risks and maximizing profitability in exploration and production, molecular analyses are essential for a deeper understanding of petroleum systems, including source rock characterization, fluids properties, thermal evolution, migration pathways, and secondary processes like biodegradation that modify oil composition.[1−3]

Traditionally, geochemical analyses of petroleum have focused on characterizing the nonpolar fraction of crude oils through techniques like liquid chromatography and gas chromatography.[4−6] However, the analysis of polar compounds, which can provide valuable complementary geochemical insights, is challenging with these methods. The advent of high-resolution spectrometry techniques, notably Fourier-transform ion cyclotron resonance mass spectrometry, FT-ICR MS, has revolutionized organic petroleum geochemistry.[7] Petroleomics now enables the identification of thousands of polar constituents of petroleum, offering potential markers to reconstruct the geochemical history of petroleum accumulations.[8−10] This molecular perspective on petroleum and reservoir fluids, alongside the chemical and mineralogical characterization of petroleum system components, plays a critical role in reducing uncertainties in oil exploration and production. FT-ICR MS, with its unparalleled mass resolution and accuracy, provides a high degree of confidence in molecular weight assignments, making it ideal for scrutinizing complex mixtures in petroleomics.[11,12]

Despite these advancements, challenges remain in applying petroleomics to petroleum organic geochemistry. In some cases, contaminants or fluids introduced during drilling or production can interfere with or compromise the accuracy of petroleomics analysis.[13,14] A viable solution is to analyze standardized fractions, particularly from the polar part of petroleum. This approach yields comparable fractions that vary only in molecular composition, enabling the constitution of robust classification models. Medium-pressure liquid chroma-

Received: June 9, 2025
Revised: September 19, 2025
Accepted: September 24, 2025
Published: October 10, 2025

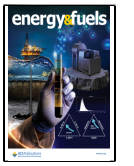

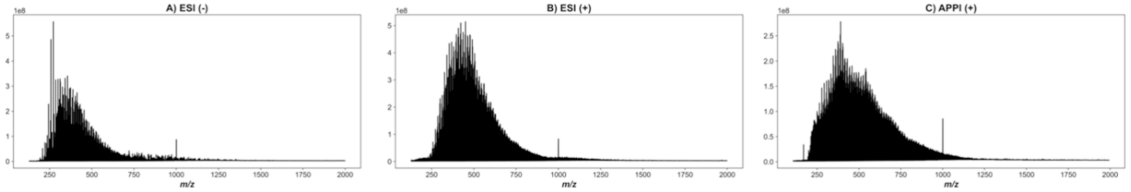

Figure 1. Representative mass spectra of a crude oil sample obtained by **A**) ESI (−); **B**) ESI (+); and **C**) APPI (+) FT-ICR-MS analyses.

tography (MPLC) offers significant potential here, as it produces highly reproducible petroleum fractions and is widely used in geochemical applications. This method uses several preparative columns to fractionate crude oils and petroleum derivatives into various subfractions based on polarity and affinity for retention on acidic and basic functionalized silica columns.[15−17]

The MPLC technique has proven effective in analyzing petroleum and its distillation cuts, significantly reducing the complexity of samples containing thousands of molecules with diverse sizes and polarities.[17] In this study, we employed H-MPLC to extract polar compounds from ten Brazilian crude oils. This approach enhances our understanding of petroleum systems by providing advanced analytical insights and detailed molecular composition data, which can inform predictions of geochemical parameters, such as formation mechanisms, thermal evolution, and origin classification.

2. EXPERIMENTAL SECTION

2.1. Materials, Reagents, and Samples. Ten Brazilian crude oil samples (**S1−S10**) from different source rocks were provided by PETROBRAS. These samples were collected from various oil fields, and no prior information regarding their biodegradation status was provided by PETROBRAS. HPLC grade solvents such as *n*-hexane (HEX), dichloromethane (DCM), and methanol (MeOH) were purchased from J. T. Baker (Phillipsburg, NJ, US) and formic acid (FA) acquired from Merck (Darmstadt, Germany) were employed to fractionate polar compounds by SPE (GX-271 ASPEC-Gilson) and H-MPLC (H-MPLC system Margot Kohnen-Willsch) techniques. For mass spectrometric analysis, high-purity methanol (HPLC grade, 99.95%) and toluene (HPLC grade, 99.9%) purchased from J. T. Baker (Phillipsburg, NJ, US) were used to dissolve all samples. Two commercial silica-packed columns (M, E) and three types of activated silica acquired from Margot Kohnen-Willsch (MKW) were utilized for SPE and H-MPLC systems. Laboratory columns (A, B, C, and D) were packed with silica (MKW) and mounted on the H-MPLC and SPE system.

2.2. Fractionation of Polar Compounds from Crude Oils by H-MPLC. The extraction of polar compounds from crude oil samples from various oil fields was performed through chromatographic fractionation using H-MPLC and online SPE, following the protocol established by Rodrigues Covas and colleagues[17] with specific adaptations. Six fractions with varying polarities and acidic/basic characteristics (low polarity-LP, low medium polarity-LMP, high medium polarity-HMP, high polarity-HP, basic-BAS, and acidic-ACD) were obtained from each fractionation.

The chromatographic system consisted of two untreated normal-phase silica columns (silica gel 60, 230−400 mesh), two base-treated silica columns (63−200 μm, 5% KOH), and one acid-treated silica column (63−200 μm, 5% HCl). The columns were dry-packed and subsequently coupled in series in the following order: untreated silica column (A), basic column (B), acidic column (C), basic column (D), and untreated column (E). Initially, 60 mg of the sample was dissolved in 1 mL of *n*-hexane and applied to column A. Subsequently, the mobile phase composed only of *n*-hexane at a flow rate of 5 mL/min was used to disperse the sample throughout the column and to collect the fraction of saturated compounds. Twenty-five mL of the saturated fraction was collected and subsequently discarded. Then, column A was coupled to the other columns arranged in sequence B, C, D, and E.

A mobile phase composed of dichloromethane and methanol (99:1, DCM/MeOH 99:1) was used to extract low- and medium-low-polarity compounds. The elution system, consisting of DCM/MeOH (99:1), was applied to column A at a flow rate of 10 mL/min, and the chromatographic system was traversed as a whole until all columns were sequentially filled. 60 mL of the first fraction, directly from column E, containing low polarity compounds, including aromatic compounds (low polarity fraction, **LP**), was collected. Immediately after the collection of the low polarity fraction, 45 mL of the low-medium polarity fraction (low,-medium polarity fraction, **LMP**) were collected, also from column E. Compounds of medium to high polarity were retained in the untreated normal phase silica column; thus, for the extraction of these, a mobile phase composed of dichloromethane and methanol 95:5 (DCM/MeOH 95:5) was used. The DCM/MeOH 95:5 system was applied to column E at a flow rate of 9 mL min^{-1}, and 45 mL of the high-medium polarity fraction (high-medium polarity fraction-**HMP**) was collected directly from column E. The HCl-functionalized silica column C (acidic column) designed for the extraction of basic compounds was isolated, and 30 mL of the basic fraction (**BAS**) were collected using the same mobile phase (DCM/MeOH 95:5). For the extraction of acidic compounds, both KOH-functionalized silica columns (columns B and D) were isolated and arranged in sequence, from which 30 mL of the acidic fraction (**ACD**) were collected using the elution system dichloromethane in acidic medium (DCM/formic acid 99:1). Finally, for the extraction of high polarity compounds (high polarity fraction-**HP**), 30 mL of the high polarity fraction was recovered directly from column A (untreated silica) via backflush using the DCM/MeOH 7:3 system. A simplified scheme of the protocol described can be seen in Figure S1. In addition, Table S1 presents the recovery for each of the six fractions obtained from ten different crude oil samples.

2.3. Molecular Characterization of Crude Oils and Their Chromatographic Fractions by ESI (±) and APPI (+) FT-ICR-MS. Mass spectrometry was conducted using a 7T SolariX 2xR FT-ICR MS (Bruker Daltonics, Bremen, Germany) equipped with both ESI and APPI sources. The instrument was calibrated daily with a solution of 0.1 μL mL^{-1} of NaTFA solution for both ionization modes across an m/z range of 150 −2000. The average calibration error ranged from 0.02 to 0.045 ppm in the linear regression mode. Samples were injected using a syringe pump at a flow rate of 120 μL h^{-1}. Data acquisition (8MW) was performed in magnitude mode over a range of m/z 150−2000 for both crude oils and fractions. Typically, for each sample, a total of 300 scans were acquired to obtain spectra with high signal/noise ratios. The raw spectra were recalibrated using Composer software, and molecular formulas were performed based on the recalibrated data.

3. RESULTS AND DISCUSSION

3.1. Molecular Characterization of Crude Oils by ESI (±) and APPI (+) FT-ICR-MS. The chemical composition of crude oil reveals critical information about its properties, including API gravity, heteroatom content (such as nitrogen and sulfur), and total acid number (TAN).[18−21] A detailed chemical analysis of crude oils and their derivatives enables inferences regarding their physicochemical properties. In this study, a comprehensive molecular analysis of ten crude oil

https://doi.org/10.1021/acs.energyfuels.5c02887
Energy Fuels 2025, 39, 20199−20212

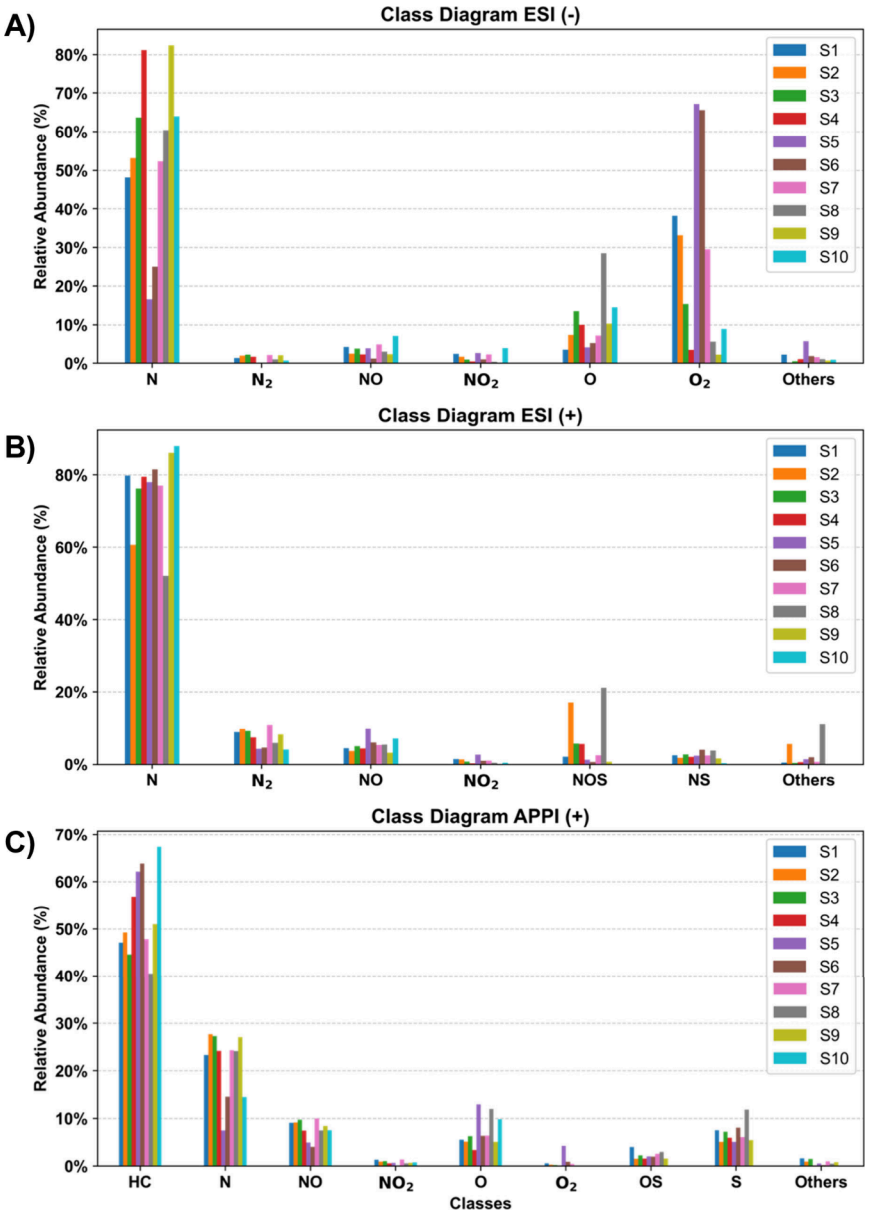

Figure 2. Class distribution diagrams for the ten crude oil samples (**S1**−**S10**) analyzed by **A**) ESI (−) FT-ICR MS, **B**) ESI (+) FT-ICR MS, and **C**) APPI (+) FT-ICR MS.

samples (**S1**−**S10**) was conducted using ESI (±) and APPI (+) FT-ICR-MS.

First, we present representative spectra obtained through ESI (±) and APPI (+) analyses (Figure 1), which are key tools for unraveling the chemical complexity of these samples. The bimodal distributions in the ESI (−) mass spectra (Figure 1A) are associated with the carbazole series, especially the benzo (DBE 12) and dibenzocarbazole (DBE 15) series, which appear in the mass range of m/z 200−350. These compounds exhibit higher ionization efficiency in ESI (−) compared to other compound classes.[22] The molecular analysis in positive ionization mode (ESI (+)) spans the same m/z range (150−1200) with prominent abundances in the region between m/z 400−600 (Figure 1B). For the spectra obtained from the APPI (+) FT-ICR MS analysis (Figure 1C), the mass ranges of the spectra comprised the m/z values from 150 to 2000, with the most prominent relative abundances in the region between m/z 300 and 800. Figures S2−S3 display the mass spectra of the ten crude oils analyzed via ESI (±) and APPI (+) FT-ICR-MS.

Figure 2 illustrates the class distribution of compounds analyzed by ESI (±) and APPI (+) FT-ICR MS across the ten crude oil samples (**S1**−**S10**). According to the data presented for ESI (−), the major components detected were nonbasic nitrogen compounds, such as indoles and carbazoles, followed by O-containing compounds, specifically those in class O_1 (one oxygen atom) and class O_2. As shown in the class distribution graphs for ESI (−) (Figure 2A), the highest detection levels of nonbasic nitrogen compounds were found in oils **S3**, **S4**, **S8**, **S9**, and **S10**. Among these samples, **S9** exhibited the highest content of N_1 species (82.41%), followed by **S4** (81.17%). In contrast, samples **S5** and **S6** showed the lowest N_1 content, with 16.56% and 25.08%, respectively. Oils **S1**, **S2**, **S5**, **S6**, and **S7** predominantly contained O_x compounds from class O_1 and O_2, with **S5** and **S6** having the highest content. For **S5**, 71.23% of the compounds accessed by ESI (−) belong to these classes,

https://doi.org/10.1021/acs.energyfuels.5c02887
Energy Fuels 2025, 39, 20199−20212

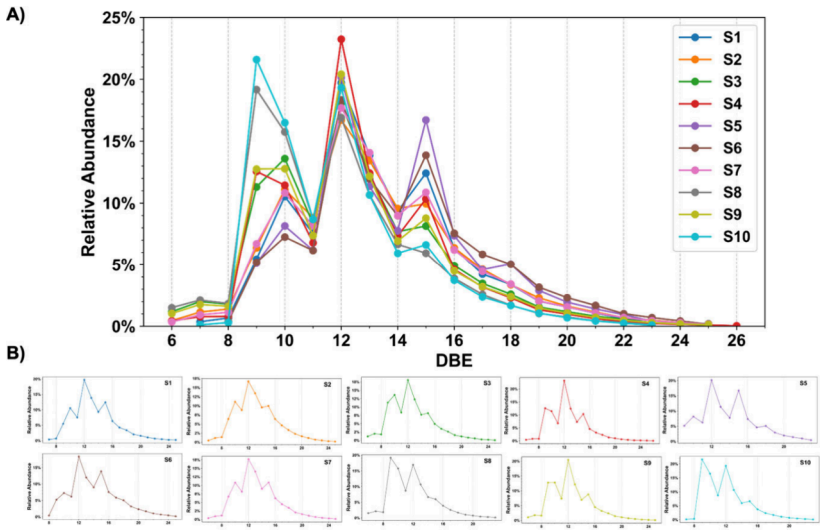

Figure 3. DBE distribution plots for the N_1 class for the ten crude oils analyzed by ESI (−) FT-ICR MS. The data are displayed in two ways: **A**) as an overlap plot for the DBE distribution for the ten oils; **B**) as an individual DBE distribution plot for each oil sample.

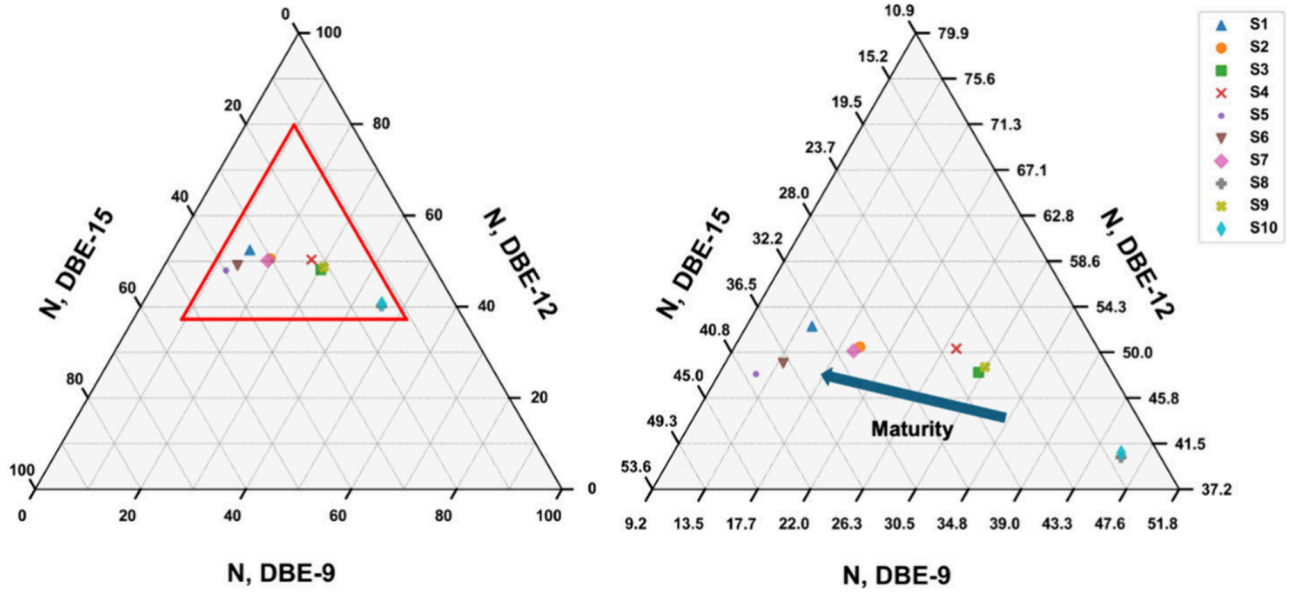

Figure 4. Ternary plots illustrating the impact of oil maturity on the relative distribution of compounds with DBE values of 9, 12, and 15. The plot on the right presents an expansion of the plot on the left to highlight subtle compositional differences.

while in **S6**, 70.92% were O_x compounds. Oils with the lowest oxygen content included **S9** (12.52%) and **S4** (13.43%). According to Ferreira and coauthors,[23] nonbasic nitrogen heterocyclic compounds are more commonly found in light and medium oils, while heavy oils exhibit a higher abundance of class O_2 compounds.

In positive ionization mode (ESI (+)), the analysis primarily detected nitrogen-containing compounds (N_1, N_2, N_1O_1, and $N_1O_1S_1$), and compounds from the N_1 class were majority detected. These compounds are correlated to basic pyridinic types. The S-containing compounds ($N_1O_1S_1$ and N_1S_1) were also identified, with a predominance of $N_1O_1S_1$ and N_1S_1 in oils **S8** and **S6**, respectively. APPI (+) analysis analyses revealed that oils **S10**, **S6**, and **S5** had the highest levels of hydrocarbons (HC class), with a relative abundance exceeding 60%. In contrast, oils **S3** and **S8** recorded the lowest levels, with a relative abundance below 45%. Regarding sulfur compounds (S_1 class and O_1S_1), they were identified as low in abundance, below 15%, with oils **S1** and **S8** exhibiting the highest relative abundances in this category. Oils **S5** and **S6** stood out for their lower levels in the classes N_1 and N_1O_1.

The relative abundance of $N_xS_xO_x$ content in the ten crude oils were evaluated, as illustrated in Figure 3. The results indicate a predominance of N-containing compounds accessed by ESI in the negative ionization mode across all samples, especially those from the N_1 class. As described in previous studies, the $N_xS_xO_x$ contents tends to change with ongoing maturation process.[24−26] Throughout the maturity progression of crude oils, N_1 class compounds are typically found in higher abundance in samples with advanced thermal maturity, whereas O_1 class compounds are predominantly detected in immature oils. This trend may be explained by the progressive depletion of O_1 compounds, accompanied by the concomitant emergence of N_1 class species.[24]

Understanding the types of N-containing compounds present in petroleum is essential, as they play a significant

https://doi.org/10.1021/acs.energyfuels.5c02887
Energy Fuels 2025, 39, 20199−20212

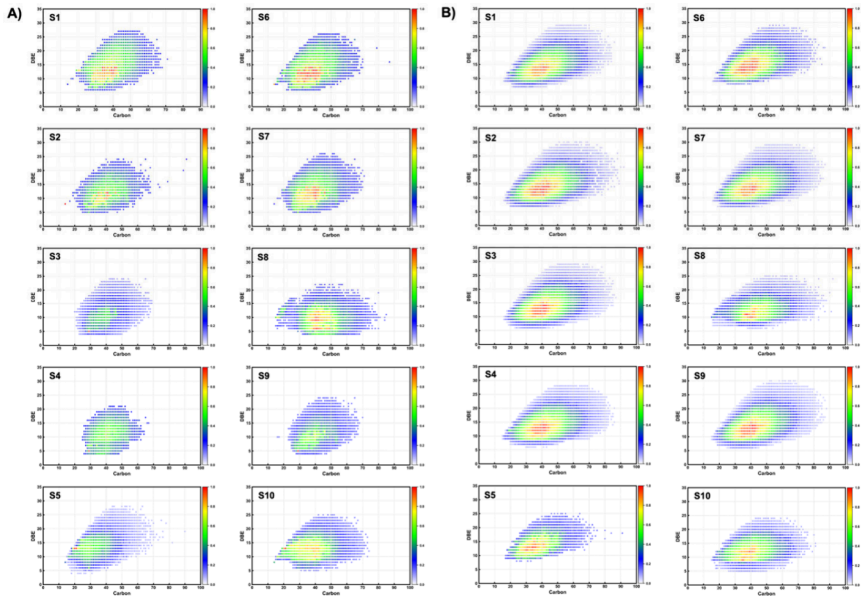

Figure 5. A) DBE versus carbon number graphs for the O class and **B)** DBE versus carbon number for the N class for the ten crude oils analyzed by APPI (+) FT-ICR MS.

role in geochemical studies, which has been consistently described.[7,24,27,28] Compounds from the N_1 class accessed by ESI in the negative ionization mode comprise predominantly alkylated pyrrolic compounds (carbazole and benzo-homologues) and other "acidic" N-containing species. This characteristic can be assessed through the parameter DBE (double bond equivalent), which can be used to determine the degree of condensation and aromaticity of a compound. The distributions of the N_1 class species analyzed in the ESI negative ion mode that are found in the crude oils are illustrated as line plots by the DBE group of species versus their relative abundance (Figure 3A and B). A general trend across the analyzed oils reveals that compounds with DBE values of 9, 12, and 15, associated with carbazole ($C_{12}H_9N$-R), benzocarbazole ($C_{16}H_{11}N$-R), and dibenzocarbazole ($C_{20}H_{13}N$-R), demonstrate higher relative abundances (%). Most of the samples show a distribution with DBE values of 6−25 and maximum relative intensities of 20% Total Monoisotopic Ion Abundances (TMIA). However, sample **S10** differs from the others, showing an absence of compounds with DBE 6, with a distribution of DBE values ranging from 7 to 23. Compounds of DBE 12 are the most abundant species in most of the oils (above 20% - TMIA), except for samples **S10** and **S8** where carbazoles with DBE 9 are identified with the greatest abundance (22% and 19 TMIA, respectively).

The relative abundance of alkylated carbazole compounds with DBE of 9 tends to decline as oil maturity increases. Simultaneously, this decrease is accompanied by a relative enrichment in compounds with DBE values greater than 12, particularly pseudo-homologues with a DBE of 15.[25−27,29] Ternary diagrams were used to evaluate changes associated with oil maturity in our sample set (Figure 4). Based on the positioning of each oil sample within the DBE 9, 12, and 15 space of the diagram, it was possible to infer a relationship between the relative variations of these three main compound groups and oil maturity. Samples **S8** and **S10** exhibit a predominant increase in the abundance of DBE of 9 species and a depletion of DBE of 15 species, suggesting that they are the least mature oil within the group. In contrast, oils **S5** and **S6** are characterized by the highest relative concentrations of DBE 15 with a decrease of DBE 9 species, showing that the core structures become more fused and aromatic with advancing thermal maturity.

DBE versus carbon number graphs were also constructed for compounds belonging to the classes of the O_1 and the O_2 (Figures S5A and B). For the O_1 class, species with DBE values ranging from 1 and 10 were detected. However, oils **S4**, **S8**, **S9**, and **S10** exhibited a reduced number of compounds, with DBE values close to 1. Regarding the carbon number distribution, compounds with carbon numbers between 18 and 40 were prevalent, except for oil S2, which displayed compounds with carbon numbers extending from 18 to 47.

In Figure S5A, DBE versus carbon number graphs for the O_1 class of the ten analyzed oils are presented. Overall, compounds with DBE values between 1 and 16 were detected, except for oil **S10**, which showed compounds with DBE values of 17. In the majority of samples, compounds with carbon numbers between 12 and 55 were detected regarding the carbon number distribution. Except for oil **S10**, compounds with carbon numbers between 12 and 62 were also detected. Figure 5B displays the DBE versus carbon number graphs for the O_2 class. Predominantly, compounds with DBE values between 1 and 15 were detected, except oils **S4** and **S9**, which presented compounds with DBE values bellow 15. Concerning the carbon number distribution, compounds with carbon numbers between 12 and 55 were majoritarian observed. Except for samples **S4** and **S9** (C_{12-40}), and **S5**, **S8**, and **S10** (C_{12-50}).

Figure 5A and B illustrates the distribution of DBE versus carbon number for the O and N classes of the ten oils analyzed by APPI (+) FT-ICR. For the O class, species with DBE values between 1 and 25 were detected, except for oils **S4** and **S8**. The number of carbons varied between 15 and 70 carbons. Regarding the N_1 class, compounds with DBE values ranging from 5 to 30 and carbon numbers ranging from 15 to 85 were detected.

The molecular composition of crude oils, specifically the distribution of heteroatom classes, can be used to infer their

https://doi.org/10.1021/acs.energyfuels.5c02887
Energy Fuels 2025, 39, 20199−20212

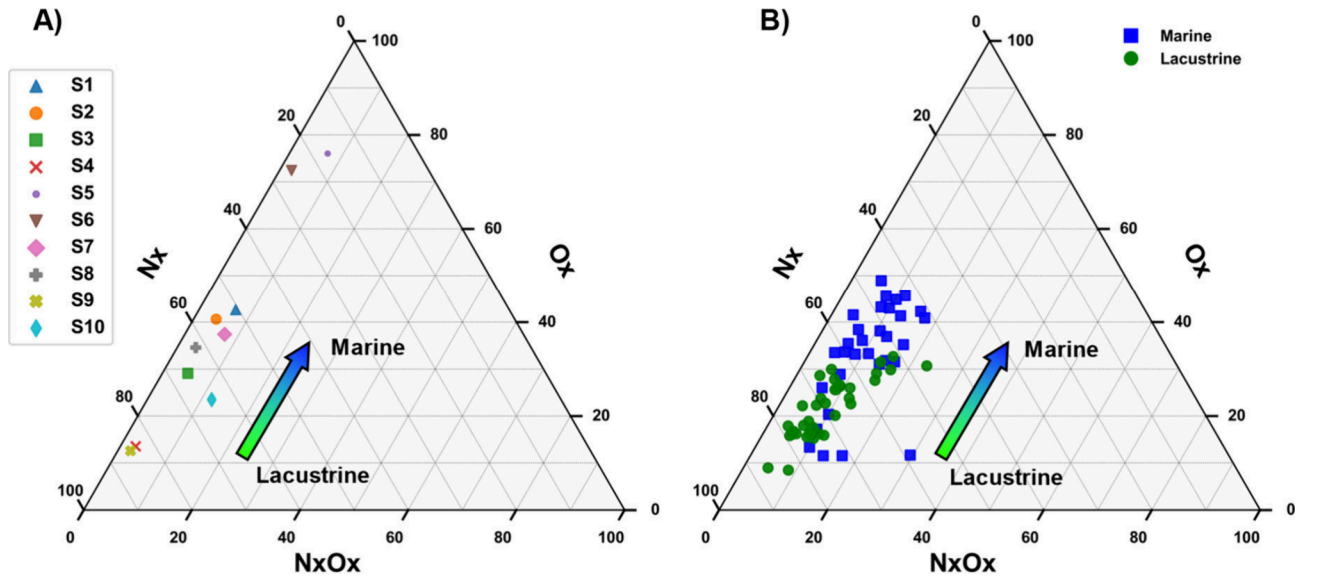

Figure 6. A) Ternary diagram for the most abundant elemental classes based on the molecular content of nitrogenous and oxygenated compounds (N_x, O_x, and N_xO_x) from ESI (−) FT-ICR-MS spectral analyses of the ten crude oil samples and **B**) comparison with the data from Rocha et al.[7] for determining lacustrine or marine origins.

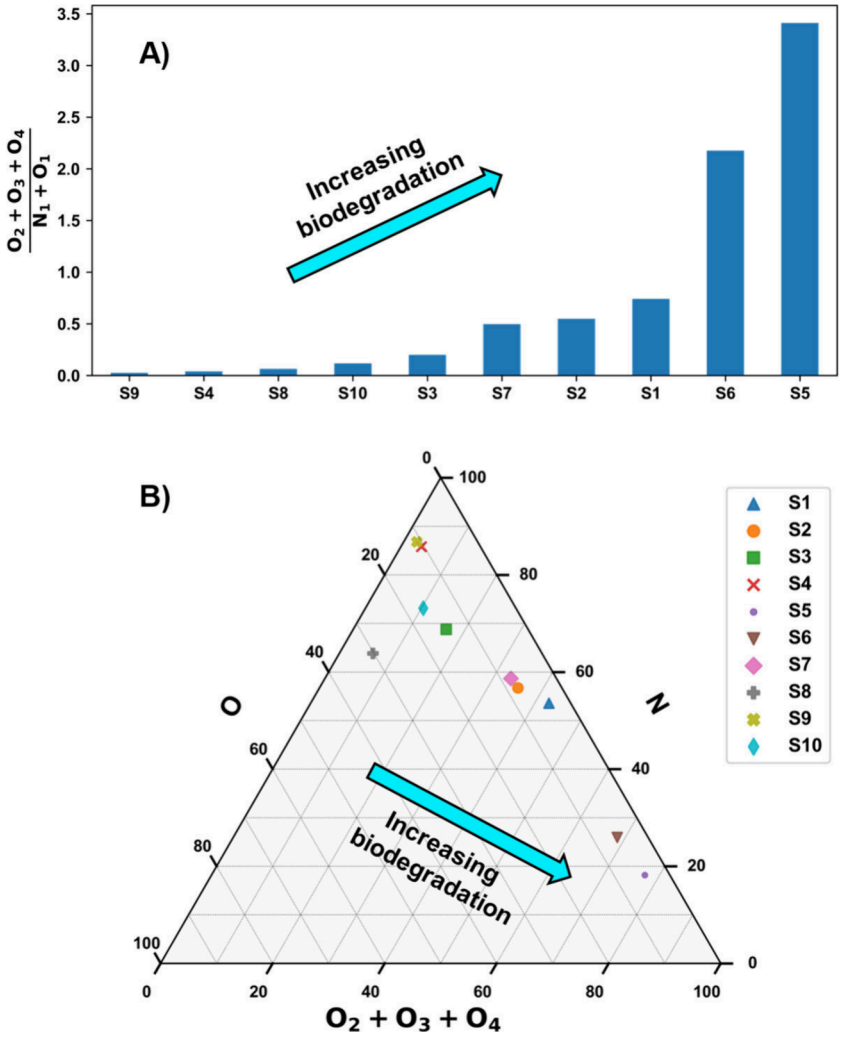

Figure 7. A) Bar chart indicating the degree of oil biodegradation based on the $(O_2 + O_3 + O_4)/(N_1 + O_1)$ ratio, which reflects the enrichment of highly oxygenated species relative to N_1 and O_1 class species; **B**) Ternary diagram showing the relative abundance of N_1, O_1 and $O_2 + O_3 + O_4$ species.

https://doi.org/10.1021/acs.energyfuels.5c02887
Energy Fuels 2025, 39, 20199−20212

origin.[7,30,31] To differentiate between lacustrine and marine oils, significant molecular differences were analyzed based on the N_x and O_x classes. Therefore, the ten crude oil samples were evaluated on the relative abundance of the three primary elemental classes: N_x, O_z, and N_xO_z, as shown in the ternary diagram (Figure 6A) and compared with the data obtained from Rocha et al. (Figure 6B).[7] According to Rocha et al.,[7] lacustrine-origin oils are typically enriched in Nx compounds (approximately 43.60−85.60%), whereas marine-origin oils tend to show lower Nx content (around 37.80−75.70%), along with a predominance of Ox compounds. Although a complete separation between lacustrine and marine origins was not achieved, the results indicate a discernible trend. For instance, samples S5 and S6 exhibit a more marine-like composition, while samples S4 and S9 are more consistent with lacustrine origin. The remaining samples appear to have transitional compositions, where both lacustrine and marine origins are equally possible.

Considering that biodegradation is one the most significant postgeneration processes that modify the oil composition, determining the molecular composition of petroleum is crucial for assessing the degree of biodegradation.[32−34] Detailed investigations of $N_xS_xO_x$ compounds constitute an effective strategy for evaluating the degree of biodegradation of crude oils. It has been reported that the relative content of species from the N_1, N_1O_1, and O_1 classes tends to decrease. In contrast, the abundance of species from the O_2, O_3, and O_4 classes tends to increase with increasing biodegradation.[35]

Based on a study by Wang and coauthors,[35] two visualization methods are presented to assess the level of biodegradation in petroleum samples: the ratio $(O_2 + O_3 + O_4)/(N_1 + O_1)$ (Figure 7A), and a ternary diagram showing the relative abundances of N_1, O_1, and $O_2 + O_3 + O_4$ (Figure 7B). These parameters allow for the evaluation of biodegradation levels, indicating that highly biodegraded samples have a propensity to transition to the amorphous $O_2 + O_3 + O_4$ species and move away from the N_1 species. This suggests a relative increase in the content of the $O_2 + O_3 + O_4$ species and a decrease in the abundance of the N_1 species as the degree of biodegradation increases. This phenomenon may be attributed to the possible formation of organic acids during the oil degradation process. The $(O_2 + O_3 + O_4)/(N_1 + O_1)$ ratio, illustrated in the bar chart (Figure 7A), serves as a reliable indicator for estimating biodegradation in crude oils. The results reveal that oil **S9** has the lowest $(O_2 + O_3 + O_4)/(N_1 + O_1)$ ratio, while oil **S5** followed by **S6** have the highest ratio, indicating varying levels of biodegradation.[35] Figure 7B displays a ternary diagram, showing the relative abundance of N_1, O_1, and $O_2 + O_3 + O_4$ species, which reflects the biodegradation level of the ten crude oils.

Wang and coauthors[35] reported that a high content of species in the O_1 class with DBE values of 4 to 7 is a characteristic of non-biodegraded oil. In contrast, heavily biodegraded oils exhibit a high species content with DBE values of 8 to 13. Figure 8 represents this approach aiming at determining the degree of biodegradation based on DBE values (8−13) for the ten crude oils. The samples of crude oils predominantly showed a high content of species with DBE values between 4 and 7, which is indicative of non-biodegraded oils. However, oils **S1**, **S2**, **S5**, **S6**, and **S7** and **S10** showed a prominent relative abundance of species with a DBE of 9.

Additionally, other properties of the oil can be determined from its molecular composition, which can significantly

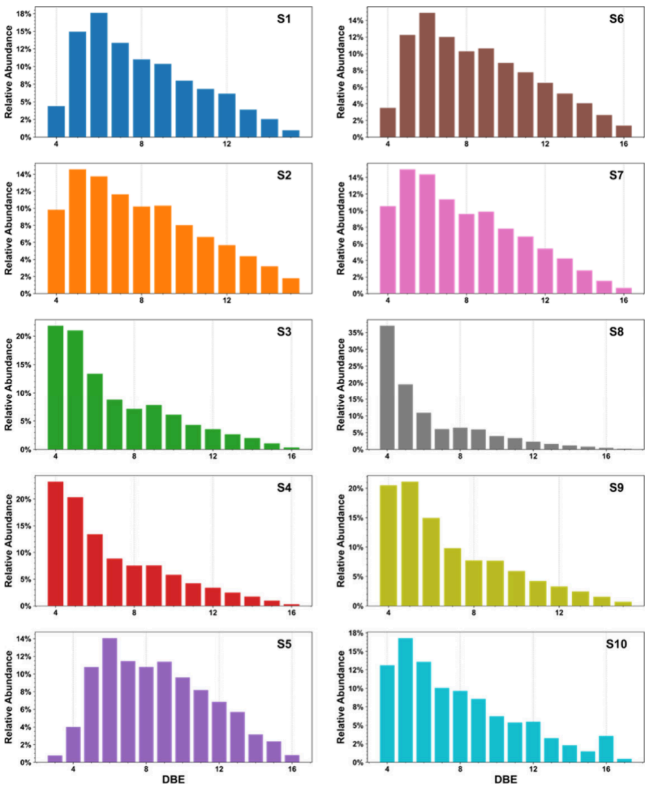

Figure 8. Distribution of the O_1 class species as a function of DBE values in the range of 4−13 for determining the degree of biodegradation of the ten crude oil samples (**S1−S10**).

influence the quality of the oil and its impact on the petroleum industry. One of these characteristics is the acidity level of the samples, which provides information about geochemical processes, such as biodegradation. In this process, hydrocarbons present in the oil are metabolized by microorganisms into carboxylic acids and other compounds.[36] Therefore, the increase in these acidic species contributes to the elevation of the acidity index. Furthermore, the carboxylic acids found in oils can also be used to estimate the level of biodegradation, which can be assessed by the A/C ratio determined between the relative abundance of linear carboxylic acids (DBE 1) and the sum of the relative abundances of cyclic acids with naphthenic nuclei (DBE 2−4).[34,36] Thus, the progress of biodegradation can be estimated by the reduction in the abundance of linear acids and an increase in the abundance of cyclic acids. Figure 9 shows the A/C index for the crude oil samples by ESI (−) FT-ICR MS, whose results indicate that oils **S1**, **S2**, **S3**, **S5**, **S6**, **S7**, and **S8** presented an A/C index < 0.2, indicating high levels of biodegradation according to Martins et al.[36] On the other hand, crude oils **S4**, **S9**, and **S10** exhibited the highest A/C values, suggesting a classification as non-biodegraded.

However, this parameter does not provide conclusive results for the acidity index of the oil and its derivatives since it considers only linear carboxylic and naphthenic acids, which are not the only classes of acids present in petroleum that can contribute to the acidity level. Therefore, to include aromatic acids (acidic compounds with DBE > 5), which also substantially contribute to the acidity level and classification of the biodegradation level of crude oils, a ternary diagram containing the abundances of linear carboxylic acids (DBE 1), naphthenic acids (DBE 2−4), and aromatic acids (DBE > 5)

https://doi.org/10.1021/acs.energyfuels.5c02887
Energy Fuels 2025, 39, 20199−20212

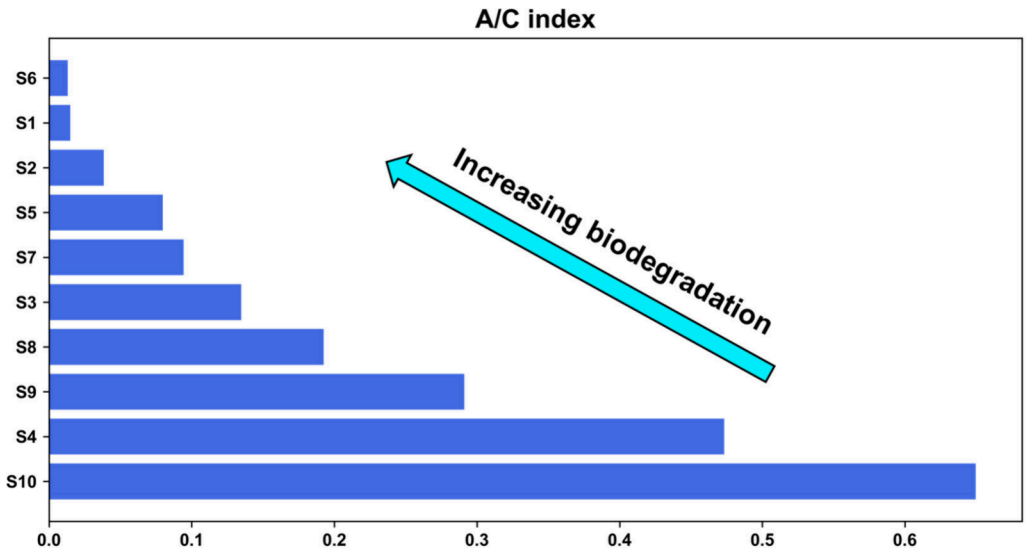

Figure 9. A/C index for the ten crude oil samples by ESI (−) FT-ICR MS analysis.

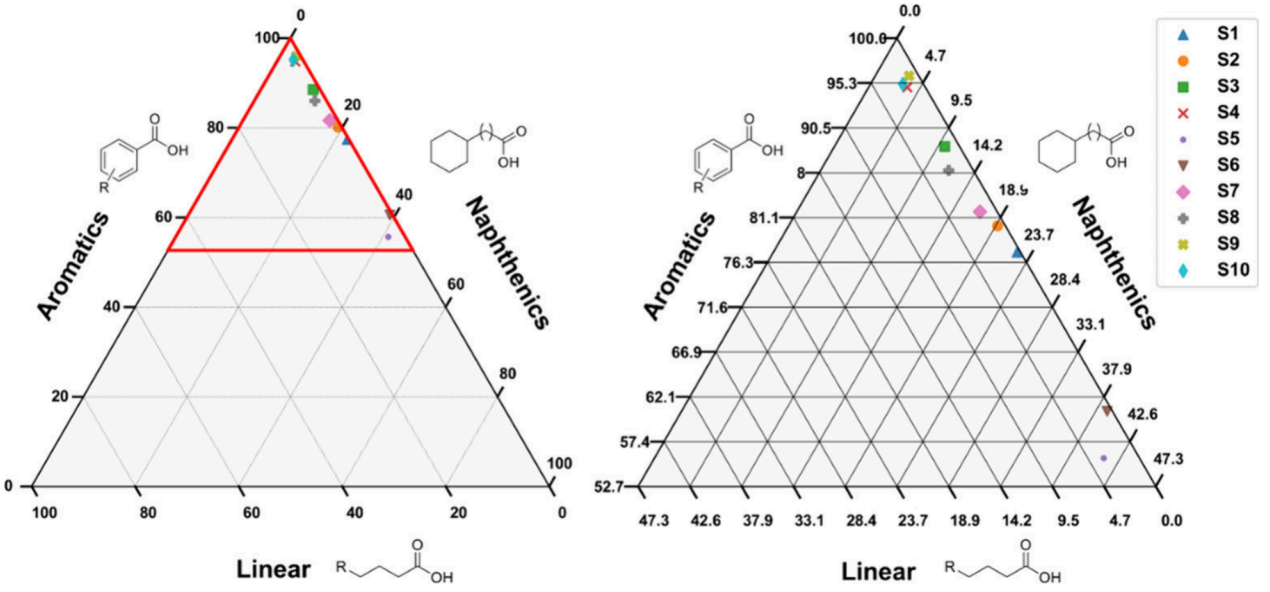

Figure 10. Ternary diagram showing the relative abundance of linear, naphthenic, and aromatic carboxylic acids for the crude oil samples analyzed by ESI (−) FT-ICR MS.

was constructed (Figure 10). The ternary diagram exhibited a significant increase in the abundance of aromatic acids (DBE > 5) in all crude oil samples and significantly low abundances of linear and aliphatic acids. There is a trend in the abundance of acids among the samples with a higher content of aromatic acids for oil **S9** and lower abundance for oil **S5**.

In addition to the compound groups previously discussed, which can be effectively used to support several geochemical interpretations such as biodegradation, thermal maturation, and origin, other classes also hold recognized importance as geochemical markers, including porphyrins.[37−40] Although porphyrins are well-established geochemical indicators, in this study they were detected only at low concentrations (<1%). For this reason, they were grouped under "other classes," while the compositional information from the more abundant compound classes was prioritized. This choice was primarily motivated by the need to elucidate the distribution of the most abundant compounds after chromatographic fractionation.

3.2. Chemical Characterization of the Fractions Obtained from Chromatographic Fractionation Using H-MPLC. Aiming to analyze the distribution of polar compounds (N_1, O_1, and S_1 classes) in the fractions obtained from chromatographic fractionation and to evaluate the effectiveness and selectivity of the functionalized stationary phases in extracting compounds with different polarities and acidic/basic characteristics, ESI (±)-FT-ICR MS analysis was performed on all fractions. However, for better comparison, only the most suitable ionization mode—based on the number of peaks and signal abundance—was used. Accordingly, the BAS, HMP, LMP, and LP fractions were analyzed in positive ionization mode, while the ACD and HP fractions were analyzed in negative ionization mode. For better visualization, a distribution of compound classes graph was constructed for each oil sample, showing the distribution of compound classes

https://doi.org/10.1021/acs.energyfuels.5c02887
Energy Fuels 2025, 39, 20199−20212

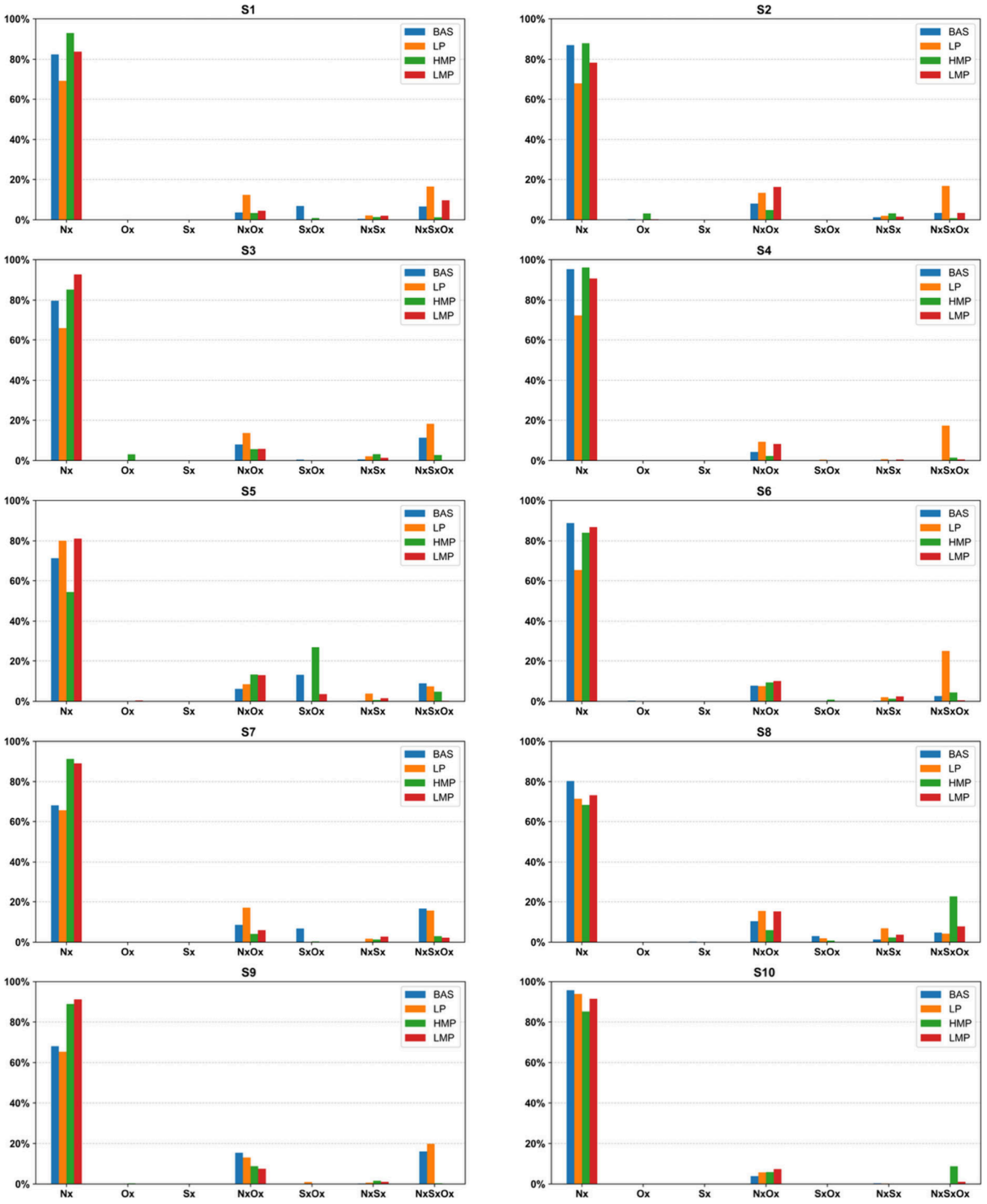

Figure 11. Distribution of compound classes in the low polarity (**LP**), low medium polarity (**LMP**), high medium polarity (**HMP**), and basic (**BAS**) fractions extracted from ten crude oil samples (**S1**−**S10**).

across the **LP**, **LMP**, **HMP**, and **BAS** fractions (positive mode) (Figure 11), and the **HP** fraction (negative mode) (Figure S6).

The results indicate a higher abundance of compounds from the Nx class across all fractions obtained in positive mode, with the Nx class being predominant in the **LMP** and **HMP**

https://doi.org/10.1021/acs.energyfuels.5c02887
Energy Fuels 2025, 39, 20199−20212

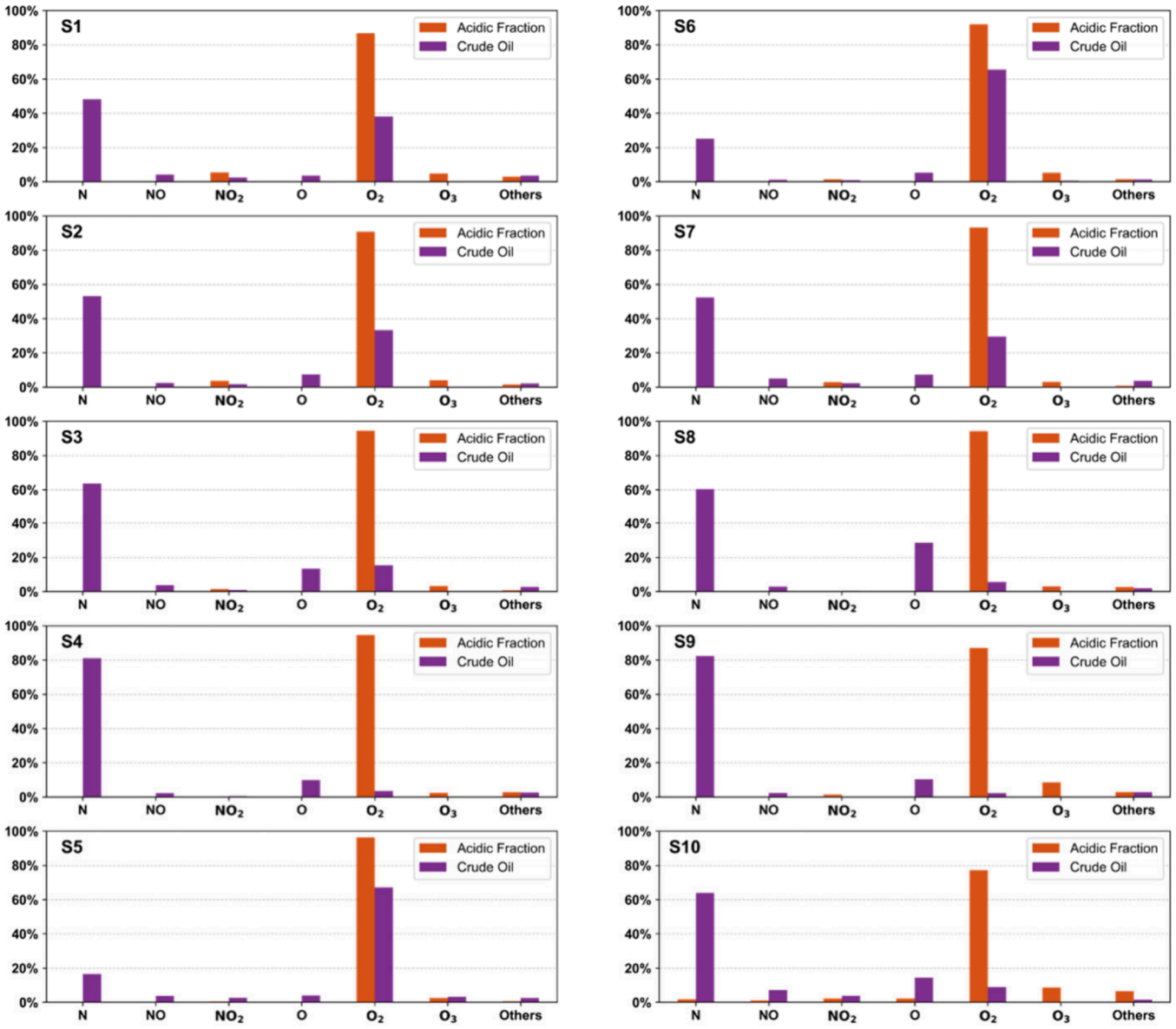

Figure 12. Distribution of compound classes in the acidic fractions and their respective oils characterized by ESI (−) FT-ICR-MS.

fractions. The NxSxOx class showed higher abundance in the **LP** fraction, while NxOx compounds were more abundant in the **BAS** fraction. All fractions exhibited similar and low abundances of the Ox, Sx, SxOx, and NxSx classes. For the **HP** fraction, which was obtained in negative ionization mode, the results indicate a higher abundance of compounds from the Ox class in most samples, followed by the NxOx and SxOx classes. The Nx class exhibited a lower abundance but remained higher than the Sx, NxSx, and NxSxOx classes, which showed consistently low levels across all samples.

Furthermore, to verify if the method employed in both techniques was able to selectively extract acidic/basic compounds and to ensure that the functionalized stationary phase and the method are capable of efficiently extracting these compounds, elemental and compound class composition analyses were performed by ESI (−) FT-ICR-MS of the ten **ACD** fractions (Figure 12). Thus, by comparing the chemical profile of the acidic fraction with the corresponding original oil, it was found that the chromatographic fractionation process was effective in extracting the O_2 class of acidic compounds in most samples, with their abundance in the fractions being approximately 90%, attesting to the remarkable efficiency of the methodology in extracting almost exclusively carboxylic acids. The resulting fraction consisted predominantly of compounds from the O_2 and the O_3 classes. In contrast, the significant presence of compounds from the N_1, N_1S_1, and N_1O_1 classes was not observed in these fractions, as expected.

The A/C index values[36] used previously to assess acidity and estimate the level of biodegradation of the oils samples can also be an important parameter to evaluate the effectiveness of extraction of linear and naphthenic acidic substances by the employed methodology, whose results showed that the acidic fractions exhibited A/C index values much higher than their corresponding oils (Figure S7). These results indicated that the fractionation concentrated predominantly linear carboxylic acids (DBE 1) in the acidic fractions as the A/C ratio was greater than 1.

To assess the effectiveness of linear and naphthenic acid extraction, heatmaps were constructed showing the distribution of the four main nuclei of aliphatic carboxylic acids for the

https://doi.org/10.1021/acs.energyfuels.5c02887
Energy Fuels 2025, 39, 20199−20212

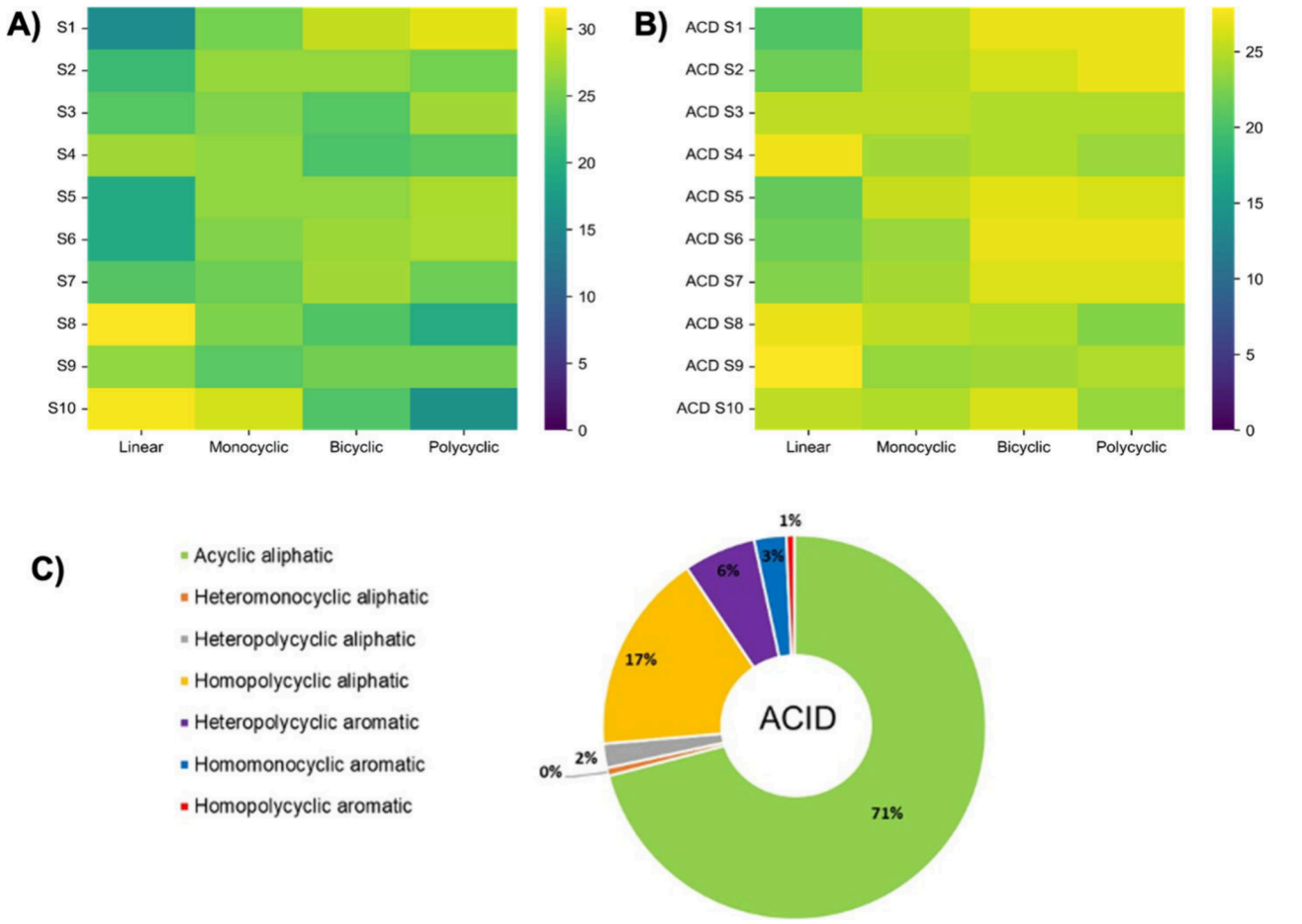

Figure 13. **A**) Heatmap displaying the distribution of the four main nuclei of aliphatic carboxylic acids for the ten crude oil samples; **B**) their corresponding acidic fractions analyzed by ESI (−) FT-ICR MS, and **C**) Overall classification based on the molecular structure of the annotated compounds from the MS/MS data of the acidic fractions obtained.

ten oils and their corresponding acidic fractions. The abundance of linear carboxylic acids (DBE 1), monocyclic (DBE 2), bicyclic (DBE 3), and polycyclic (DBE ≥ 4) was compared in the oils and their corresponding acidic fractions (Figure 13A). The results indicate that acid extraction was successfully performed in all fractionations as the relative intensity of all classes increased significantly in the fractions compared to the crude oils. Oil **S8** exhibited a higher relative intensity of linear carboxylic acids, while oil **S2** showed a greater abundance of polycyclic carboxylic acids. Oils **S10** and **S8** displayed a prominence in the monocyclic acid class (Figure 13B).

In silico dereplication approaches and data mining tools (Classical Molecular Networking—MN,[41] Dereplicator+,[42] Network Annotation Propagation—NAP,[43] Moldiscovery,[44] MS2LDA,[45] MolNetEnhancer[46]) were applied to the MS/MS spectral data set to dereplicate the acidic fractions and annotate the most abundant compounds in these fractions. The data mining and chemical classification tools were used to determine the chemical classes, whose results showed a predominant composition of acyclic aliphatic structures (71%), followed by homopolycyclic aliphatic (17%) and heteropolycyclic aromatic (9%) structures (Figure 13C). A more comprehensive characterization allowed for a more refined classification at the subclass level, with the majority annotated as long- and very-long-chain carboxylic acids and derivatives (72%). The absence of other compound classes attests to the efficiency of the extraction methodology in obtaining fractions abundant in acidic constituents. Additionally, the molecular structures of dozens of O_2 class carboxylic acids were assigned through MS/MS fragmentation data. The proposed structures, classification (linear, naphthenic, and aromatic), and molecular data (exact mass, empirical formula, and number of DBE) of the annotated acidic compounds are described in Table S3.

4. CONCLUSIONS

The results obtained in this study demonstrate the potential of combining ultrahigh-resolution mass spectrometry with separation techniques for determining geochemical processes. The chemical characterization of crude oils using FT-ICR MS enabled the determination of biodegradation levels, thermal evolution, acidity index, and oil origin through the molecular content of the N_x, O_x, and S_x classes. The relative abundance of polar compounds (N_x, O_x, and S_x) was evaluated in ten crude oils to assess thermal evolution, with the results showing a predominance of nitrogen compounds in all samples and a low abundance of sulfur compounds. To predict whether the oil's origin was lacustrine or marine, molecular differences in the N_x and O_x classes were analyzed. Although complete discrimination of the crude oil origins was not achieved, the results indicated a tendency toward separation with four samples clearly distinguished and six remaining within an unresolved cluster. The relative abundances of N_1, O_1, and O_2−O_4 classes,

https://doi.org/10.1021/acs.energyfuels.5c02887
Energy Fuels 2025, 39, 20199−20212

the $(O_2 + O_3 + O_4)/(N_1 + O_1)$ ratio, and the A/C index were used as indicators of biodegradation levels. The A/C index indicated that crude oils S4, S9, and S10 are nonbiodegraded, while S6, S1, S2, S5, and S7 show varying degrees of biodegradation. This classification is further supported by the $(O_2 + O_3 + O_4)/(N_1 + O_1)$ ratio, which suggests biodegradation in crude oils S5 and S6. Ternary diagrams showed that crude oils S8 and S10 have higher DBE of 9 and lower DBE of 15 abundances, indicating lower maturity, while S5 and S6 exhibit higher DBE of 15 and lower DBE of 9, reflecting advanced thermal maturity. Overall, the combination of this separation methodology with the molecular characterization of polar compounds using FT-ICR MS offers a promising approach for geochemical evaluations of crude oils and source rocks.

■ ASSOCIATED CONTENT

Data Availability Statement

Data will be made available on request.

Supporting Information

The Supporting Information is available free of charge at https://pubs.acs.org/doi/10.1021/acs.energyfuels.5c02887.

Schematic representation for extracting polar compounds from crude oil samples using H-MPLC system; mass spectra of crude oil samples by ESI (±) and APPI (+) FT-ICR-MS; A/C index for the ten crude oil samples and corresponding acidic fractions; FT-ICR-MS instrument and measurement parameters; and molecular data of acidic compounds obtained using in silico dereplication (PDF)

■ AUTHOR INFORMATION

Corresponding Author

Boniek Gontijo − *Federal University of Goiás (UFG), Chemistry Institute, 74690 900 Goiânia, Goiás, Brazil;* orcid.org/0000-0003-1197-4284; Email: boniek@ufg.br

Authors

Nerilson Marques Lima − *Federal University of Goiás (UFG), Chemistry Institute, 74690 900 Goiânia, Goiás, Brazil;* orcid.org/0000-0001-9669-0306

Hugo Gontijo Machado − *Federal University of Goiás (UFG), Chemistry Institute, 74690 900 Goiânia, Goiás, Brazil*

Gesiane da Silva Lima − *Federal University of Goiás (UFG), Chemistry Institute, 74690 900 Goiânia, Goiás, Brazil*

Joveilton Batista da Silva Junior − *Federal University of Goiás (UFG), Chemistry Institute, 74690 900 Goiânia, Goiás, Brazil*

Juliene Aljahara Sousa Cardoso − *Federal University of Goiás (UFG), Chemistry Institute, 74690 900 Goiânia, Goiás, Brazil*

Gabriel Franco dos Santos − *Federal University of Goiás (UFG), Chemistry Institute, 74690 900 Goiânia, Goiás, Brazil*

Andrea Rodrigues Chaves − *Federal University of Goiás (UFG), Chemistry Institute, 74690 900 Goiânia, Goiás, Brazil;* orcid.org/0000-0002-1600-1660

Rodrigo Cabral da Silva − *Division of Geochemistry, Petrobras Research and Development Center (CENPES), 21941-915 Rio de Janeiro, RJ, Brazil*

Alexandre de Andrade Ferreira − *Division of Geochemistry, Petrobras Research and Development Center (CENPES), 21941-915 Rio de Janeiro, RJ, Brazil;* orcid.org/0000-0001-6257-960X

Complete contact information is available at: https://pubs.acs.org/10.1021/acs.energyfuels.5c02887

Author Contributions

Nerilson Marques Lima: Methodology, Data curation, Writing - original draft, Visualization. Gesiane da Silva Lima: Methodology, Data curation, Writing - review and editing, Validation, Visualization. Hugo Gontijo Machado: Data curation, Validation, Visualization. Andréa Rodrigues Chaves: Writing - review and editing, Visualization. Joveilton Batista da Silva Junior: Methodology. Gabriel Franco dos Santos: Methodology, Writing - review and editing, Visualization. Rodrigo Cabral da Silva: Methodology, Writing - review and editing, Visualization, Funding acquisition. Boniek Gontijo Vaz: Conceptualization, Writing - review and editing, Resources, Supervision, Project administration.

Funding

The Article Processing Charge for the publication of this research was funded by the Coordenacao de Aperfeicoamento de Pessoal de Nivel Superior (CAPES), Brazil (ROR identifier: 00x0ma614).

Notes

The authors declare no competing financial interest.

■ ACKNOWLEDGMENTS

The authors acknowledge financial support from Petróleo Brasileiro SA- Petrobras, CNPq, CAPES and FAPEG. We also acknowledge the Geochemistry Laboratory from the Petrobras Research and Development Center (CENPES).

■ REFERENCES

(1) Peters, K. E.; Walters, C. C.; Moldowan, J. M. *The Biomarker Guide: Biomarkers and Isotopes in the Environment and Human History*, 2nd ed.; Cambridge University Press, 2007; Vol. 2.

(2) Noah, M.; Horsfield, B.; Han, S.; Wang, C. Precise Maturity Assessment over a Broad Dynamic Range Using Polycyclic and Heterocyclic Aromatic Compounds. *Org. Geochem.* **2020**, *148*, 104099.

(3) Wang, D.; Li, M.; Cheng, D.; Du, Y.; Shi, Q.; Zou, X.; Chen, Q. New Biodegradation Degree Proxies Based on Acids and Neutral Nitrogen- and Oxygen-Containing Compounds Characterized by High Resolution Mass Spectrometry. *Fuel* **2023**, *347*, 128438.

(4) Kim, E.; Cho, E. J.; Moon, S.; Park, J., Il; Kim, S. Characterization of Petroleum Heavy Oil Fractions Prepared by Preparatory Liquid Chromatography with Thin-Layer Chromatography, High-Resolution Mass Spectrometry, and Gas Chromatography with an Atomic Emission Detector. *Energy Fuels* **2016**, *30* (4), 2932−2940.

(5) Pollo, B. J.; Alexandrino, G. L.; Augusto, F.; Hantao, L. W. The Impact of Comprehensive Two-Dimensional Gas Chromatography on Oil & Gas Analysis: Recent Advances and Applications in Petroleum Industry. *TrAC - Trends in Analytical Chemistry* **2018**, *105*, 202−217.

(6) Karevan, A.; Zirrahi, M.; Hassanzadeh, H. Standardized High-Performance Liquid Chromatography to Replace Conventional Methods for Determination of Saturate, Aromatic, Resin, and Asphaltene (SARA) Fractions. *ACS Omega* **2022**, *7* (22), 18897−18903.

(7) dos Santos Rocha, Y.; Pereira, R. C. L.; Mendonça Filho, J. G. Geochemical Characterization of Lacustrine and Marine Oils from Off-Shore Brazilian Sedimentary Basins Using Negative-Ion Electro-

spray Fourier Transform Ion Cyclotron Resonance Mass Spectrometry (ESI FTICR-MS). *Org. Geochem.* **2018**, *124*, 29−45.
(8) Marshall, A. G.; Rodgers, R. P. Petroleomics: Chemistry of the Underworld. *Proc. Natl. Acad. Sci. U. S. A.* **2008**, *105* (47), 18090−18095.
(9) Comisarow, M. B.; Marshall, A. G. Fourier Transform Ion Cyclotron Resonance Spectroscopy. *Chem. Phys. Lett.* **1974**, *25* (2), 282−283.
(10) Xian, F.; Hendrickson, C. L.; Marshall, A. G. High Resolution Mass Spectrometry. *Anal. Chem.* **2012**, *84* (2), 708−719.
(11) Barros, E. V.; Dias, H. P.; Pinto, F. E.; Gomes, A. O.; Moura, R. R.; Neto, A. C.; Freitas, J. C. C.; Aquije, G. M. F. V.; Vaz, B. G.; Romão, W. Characterization of Naphthenic Acids in Thermally Degraded Petroleum by ESI(−)-FT-ICR MS and 1H NMR after Solid-Phase Extraction and Liquid/Liquid Extraction. *Energy Fuels* **2018**, *32* (3), 2878−2888.
(12) Barrow, M. P.; Peru, K. M.; McMartin, D. W.; Headley, J. V. Effects of Extraction PH on the Fourier Transform Ion Cyclotron Resonance Mass Spectrometry Profiles of Athabasca Oil Sands Process Water. *Energy Fuels* **2016**, *30* (5), 3615−3621.
(13) Ventura, G. T.; Raghuraman, B.; Nelson, R. K.; Mullins, O. C.; Reddy, C. M. Compound Class Oil Fingerprinting Techniques Using Comprehensive Two-Dimensional Gas Chromatography (GC × GC). *Org. Geochem.* **2010**, *41* (9), 1026−1035.
(14) Santos, J. M.; Galaverna, R. de S.; Pudenzi, M. A.; Schmidt, E. M.; Sanders, N. L.; Kurulugama, R. T.; Mordehai, A.; Stafford, G. C.; Wisniewski, A.; Eberlin, M. N. Petroleomics by Ion Mobility Mass Spectrometry: Resolution and Characterization of Contaminants and Additives in Crude Oils and Petrofuels. *Analytical Methods* **2015**, *7* (11), 4450−4463.
(15) Willsch, H.; Clegg, H.; Horsfield, B.; Radke, M.; Wilkes, H. Liquid Chromatographic Separation of Sediment, Rock, and Coal Extracts and Crude Oil into Compound Classes. *Anal. Chem.* **1997**, *69* (20), 4203−4209.
(16) Radke, M.; Willsch, H.; Welte, D. H. Preparative Hydrocarbon Group Type Determination by Automated Medium Pressure Liquid Chromatography. *Anal. Chem.* **1980**, *52* (3), 406−411.
(17) Rodrigues Covas, T.; Santos de Freitas, C.; Valadares Tose, L.; Valencia-Dávila, J. A.; dos Santos Rocha, Y.; Duncan Rangel, M.; Cabral da Silva, R.; Gontijo Vaz, B. Fractionation of Polar Compounds from Crude Oils by Hetero-Medium Pressure Liquid Chromatography (H-MPLC) and Molecular Characterization by Ultrahigh-Resolution Mass Spectrometry. *Fuel* **2020**, *267*, 117289.
(18) Young, R. E. Petroleum Refining Process Control and Real-Time Optimization. *IEEE Control Syst.* **2006**, *26* (6), 73−83.
(19) de Aguiar, D. V. A.; Lima, G. d. S.; Roque, J. V.; Oliveira, J. V. A.; Medeiros Junior, I.; Gomes, A. d. O.; Mendes, L. A. N.; Vaz, B. G. Quantitative Evaluation of Non-Basic Nitrogen-Containing Compounds in Petroleum-Derived Samples by Direct Injection ESI (−) Orbitrap MS? *Anal. Chem.* **2023**, *95*, 6507−6513.
(20) Roque, J. V.; Cardoso, W. J.; de Aguiar, D. V. A.; dos Santos, G. F.; Gomes, A. de O.; Medeiros Júnior, I.; Lima, G. da S.; Gontijo, B. Integrating FT-ICR MS and Machine Learning to Forecast Acid Content Across Boiling Cuts. *Anal. Chem.* **2025**, *97* (11), 5965−5974.
(21) Hur, M.; Yeo, I.; Kim, E.; No, M.; Koh, J.; Cho, Y. J.; Lee, J. W.; Kim, S. Correlation of FT-ICR Mass Spectra with the Chemical and Physical Properties of Associated Crude Oils. *Energy Fuels* **2010**, *24* (10), 5524−5532.
(22) Cho, E.; Witt, M.; Hur, M.; Jung, M. J.; Kim, S. Application of FT-ICR MS Equipped with Quadrupole Detection for Analysis of Crude Oil. *Anal. Chem.* **2017**, *89* (22), 12101−12107.
(23) Ferreira, P. S.; Madeira, N. C. L.; Folli, G. S.; Romão, W.; Filgueiras, P. R.; Kuster, R. M. SAP Fractions from Light, Medium and Heavy Oils: Correlation between Chemical Profile and Stationary Phases. *Fuel* **2020**, *274* (April), 117866.
(24) Poetz, S.; Horsfield, B.; Wilkes, H. Maturity-Driven Generation and Transformation of Acidic Compounds in the Organic-Rich Posidonia Shale as Revealed by Electrospray Ionization Fourier Transform Ion Cyclotron Resonance Mass Spectrometry. *Energy Fuels* **2014**, *28* (8), 4877−4888.
(25) Oldenburg, T. B. P.; Brown, M.; Bennett, B.; Larter, S. R. The Impact of Thermal Maturity Level on the Composition of Crude Oils, Assessed Using Ultra-High Resolution Mass Spectrometry. *Org. Geochem.* **2014**, *75*, 151−168.
(26) Wang, D.; Li, M.; Chen, J.; Chen, H.; Shi, Q. A New Ternary Diagram to Decipher the Evolution of Maturity and Biodegradation of Crude Oil Using ESI FT-ICR MS. *Fuel* **2024**, *359*, 130499.
(27) Martins, L. L.; Schulz, H.-M.; Noah, M.; Poetz, S.; Severiano Ribeiro, H. J. P.; da Cruz, G. F. New Paleoenvironmental Proxies for the Irati Black Shales (Paraná Basin, Brazil) Based on Acidic NSO Compounds Revealed by Ultra-High Resolution Mass Spectrometry. *Org. Geochem.* **2021**, *151*, 104152.
(28) SNYDER, L. R. Distribution of Benzcarbazole Isomers in Petroleum as Evidence for Their Biogenic Origin. *Nature* **1965**, *205* (4968), 277−277.
(29) Ziegs, V.; Horsfield, B.; Noah, M.; Poetz, S.; Hartwig, A.; Rinna, J.; Skeie, J. E. Unravelling Maturity- and Migration-Related Carbazole and Phenol Distributions in Central Graben Crude Oils. *Mar Pet Geol* **2018**, *94*, 114−130.
(30) Melendez-Perez, J. J.; Campos Oliveira, L. F.; Miranda, N.; Sussulini, A.; Eberlin, M. N.; Bastos, W. L.; Rangel, M. D.; dos Santos Rocha, Y. Lacustrine versus Marine Oils: Fast and Accurate Molecular Discrimination via Electrospray Fourier Transform Ion Cyclotron Resonance Mass Spectrometry and Multivariate Statistics. *Energy Fuels* **2020**, *34* (8), 9222−9230.
(31) dos Santos Rocha, Y.; Pereira, R. C. L.; Mendonça Filho, J. G. Geochemical Assessment of Oils from the Mero Field, Santos Basin, Brazil. *Org. Geochem.* **2019**, *130*, 1−13.
(32) Vaz, B. G.; Silva, R. C.; Klitzke, C. F.; Simas, R. C.; Lopes Nascimento, H. D.; Pereira, R. C. L.; Garcia, D. F.; Eberlin, M. N.; Azevedo, D. A. Assessing Biodegradation in the Llanos Orientales Crude Oils by Electrospray Ionization Ultrahigh Resolution and Accuracy Fourier Transform Mass Spectrometry and Chemometric Analysis. *Energy Fuels* **2013**, *27* (3), 1277−1284.
(33) Liu, Y.; Wan, Y. Y.; Zhu, Y.; Fei, C.; Shen, Z.; Ying, Y. Impact of Biodegradation on Polar Compounds in Crude Oil: Comparative Simulation of Biodegradation from Two Aerobic Bacteria Using Ultrahigh-Resolution Mass Spectrometry. *Energy Fuels* **2020**, *34* (5), 5553−5565.
(34) Hughey, C. A.; Galasso, S. A.; Zumberge, J. E. Detailed Compositional Comparison of Acidic NSO Compounds in Biodegraded Reservoir and Surface Crude Oils by Negative Ion Electrospray Fourier Transform Ion Cyclotron Resonance Mass Spectrometry. *Fuel* **2007**, *86* (5−6), 758−768.
(35) Wang, D.; Li, M.; Cheng, D.; Du, Y.; Shi, Q.; Zou, X.; Chen, Q. New Biodegradation Degree Proxies Based on Acids and Neutral Nitrogen- and Oxygen-Containing Compounds Characterized by High Resolution Mass Spectrometry. *Fuel* **2023**, *347*, 128438.
(36) Martins, L. L.; Pudenzi, M. A.; da Cruz, G. F.; Nascimento, H. D. L.; Eberlin, M. N. Assessing Biodegradation of Brazilian Crude Oils via Characteristic Profiles of O 1 and O 2 Compound Classes: Petroleomics by ESI (−) FT-ICR Mass Spectrometry. *Energy Fuels* **2017**, *31* (7), 6649−6657.
(37) McKenna, A. M.; Purcell, J. M.; Rodgers, R. P.; Marshall, A. G. Identification of Vanadyl Porphyrins in a Heavy Crude Oil and Raw Asphaltene by Atmospheric Pressure Photoionization Fourier Transform Ion Cyclotron Resonance (FT-ICR) Mass Spectrometry. *Energy Fuels* **2009**, *23* (4), 2122−2128.
(38) Ramírez-Pradilla, J. S.; Blanco-Tirado, C.; Hubert-Roux, M.; Giusti, P.; Afonso, C.; Combariza, M. Y. Comprehensive Petroporphyrin Identification in Crude Oils Using Highly Selective Electron Transfer Reactions in MALDI-FTICR-MS. *Energy Fuels* **2019**, *33* (5), 3899−3907.
(39) Zheng, F.; Yang, W.; Wang, Y.; An, M.; Huo, D.; Wang, C.; Cao, Q.; He, J.; Shi, Q.; Sun, Y. Identification of Novel Sulfur-Containing Petroporphyrins in a Natural Bitumen: Potential Biomarkers for Aerobic Organisms. *Org. Geochem.* **2025**, *204*, 104987.

https://doi.org/10.1021/acs.energyfuels.5c02887
Energy Fuels 2025, 39, 20199−20212

(40) McKenna, A. M.; Williams, J. T.; Putman, J. C.; Aeppli, C.; Reddy, C. M.; Valentine, D. L.; Lemkau, K. L.; Kellermann, M. Y.; Savory, J. J.; Kaiser, N. K.; Marshall, A. G.; Rodgers, R. P. Unprecedented Ultrahigh Resolution FT-ICR Mass Spectrometry and Parts-Per-Billion Mass Accuracy Enable Direct Characterization of Nickel and Vanadyl Porphyrins in Petroleum from Natural Seeps. *Energy Fuels* **2014**, *28* (4), 2454−2464.
(41) Wang, M.; Carver, J. J.; Phelan, V. V.; Sanchez, L. M.; Garg, N.; Peng, Y.; Nguyen, D. D.; Watrous, J.; Kapono, C. A.; Luzzatto-Knaan, T.; Porto, C.; Bouslimani, A.; Melnik, A. V.; Meehan, M. J.; Liu, W. T.; Crüsemann, M.; Boudreau, P. D.; Esquenazi, E.; Sandoval-Calderón, M.; Kersten, R. D.; Pace, L. A.; Quinn, R. A.; Duncan, K. R.; Hsu, C. C.; Floros, D. J.; Gavilan, R. G.; Kleigrewe, K.; Northen, T.; Dutton, R. J.; Parrot, D.; Carlson, E. E.; Aigle, B.; Michelsen, C. F.; Jelsbak, L.; Sohlenkamp, C.; Pevzner, P.; Edlund, A.; McLean, J.; Piel, J.; Murphy, B. T.; Gerwick, L.; Liaw, C. C.; Yang, Y. L.; Humpf, H. U.; Maansson, M.; Keyzers, R. A.; Sims, A. C.; Johnson, A. R.; Sidebottom, A. M.; Sedio, B. E.; Klitgaard, A.; Larson, C. B.; Boya P, C. A.; Torres-Mendoza, D.; Gonzalez, D. J.; Silva, D. B.; Marques, L. M.; Demarque, D. P.; Pociute, E.; O'Neill, E. C.; Briand, E.; Helfrich, E. J. N.; Granatosky, E. A.; Glukhov, E.; Ryffel, F.; Houson, H.; Mohimani, H.; Kharbush, J. J.; Zeng, Y.; Vorholt, J. A.; Kurita, K. L.; Charusanti, P.; McPhail, K. L.; Nielsen, K. F.; Vuong, L.; Elfeki, M.; Traxler, M. F.; Engene, N.; Koyama, N.; Vining, O. B.; Baric, R.; Silva, R. R.; Mascuch, S. J.; Tomasi, S.; Jenkins, S.; Macherla, V.; Hoffman, T.; Agarwal, V.; Williams, P. G.; Dai, J.; Neupane, R.; Gurr, J.; Rodríguez, A. M. C.; Lamsa, A.; Zhang, C.; Dorrestein, K.; Duggan, B. M.; Almaliti, J.; Allard, P. M.; Phapale, P.; Nothias, L. F.; Alexandrov, T.; Litaudon, M.; Wolfender, J. L.; Kyle, J. E.; Metz, T. O.; Peryea, T.; Nguyen, D. T.; VanLeer, D.; Shinn, P.; Jadhav, A.; Müller, R.; Waters, K. M.; Shi, W.; Liu, X.; Zhang, L.; Knight, R.; Jensen, P. R.; Palsson, B.; Pogliano, K.; Linington, R. G.; Gutiérrez, M.; Lopes, N. P.; Gerwick, W. H.; Moore, B. S.; Dorrestein, P. C.; Bandeira, N. Sharing and Community Curation of Mass Spectrometry Data with Global Natural Products Social Molecular Networking. *Nat. Biotechnol.* **2016**, *34* (8), 828−837.
(42) Mohimani, H.; Gurevich, A.; Shlemov, A.; Mikheenko, A.; Korobeynikov, A.; Cao, L.; Shcherbin, E.; Nothias, L. F.; Dorrestein, P. C.; Pevzner, P. A. Dereplication of Microbial Metabolites through Database Search of Mass Spectra. *Nat. Commun.* **2018**, *9* (1), 1−12.
(43) da Silva, R. R.; Wang, M.; Nothias, L. F.; van der Hooft, J. J. J.; Caraballo-Rodríguez, A. M.; Fox, E.; Balunas, M. J.; Klassen, J. L.; Lopes, N. P.; Dorrestein, P. C. Propagating Annotations of Molecular Networks Using in Silico Fragmentation. *PLoS Comput. Biol.* **2018**, *14* (4), e1006089.
(44) Cao, L.; Guler, M.; Tagirdzhanov, A.; Lee, Y. Y.; Gurevich, A.; Mohimani, H. MolDiscovery: Learning Mass Spectrometry Fragmentation of Small Molecules. *Nat. Commun.* **2021**, *12* (1), 1−13.
(45) Van Der Hooft, J. J. J.; Wandy, J.; Barrett, M. P.; Burgess, K. E. V.; Rogers, S. Topic Modeling for Untargeted Substructure Exploration in Metabolomics. *Proc. Natl. Acad. Sci. U. S. A.* **2016**, *113* (48), 13738−13743.
(46) Ernst, M.; Kang, K. B.; Caraballo-Rodríguez, A. M.; Nothias, L. F.; Wandy, J.; Chen, C.; Wang, M.; Rogers, S.; Medema, M. H.; Dorrestein, P. C.; van der Hooft, J. J. J. Molnetenhancer: Enhanced Molecular Networks by Integrating Metabolome Mining and Annotation Tools. *Metabolites* **2019**, *9* (7), 144.

https://doi.org/10.1021/acs.energyfuels.5c02887
Energy Fuels 2025, 39, 20199−20212